NASA
Technical Memorandum 107451

Army Research Laboratory
Technical Report ARL–TR–1370

Computerized Simulation of Meshing of Conventional Helical Involute Gears and Modification of Geometry

F.L. Litvin and J. Lu
University of Illinois at Chicago
Chicago, Illinois

D.P. Townsend
Lewis Research Center
Cleveland, Ohio

M. Hawkins
Allison Engine Company
Indianapolis, Indiana

July 1997

National Aeronautics and
Space Administration

COMPUTERIZED SIMULATION OF MESHING OF CONVENTIONAL HELICAL INVOLUTE GEARS AND MODIFICATION OF GEOMETRY

F.L. Litvin* **and J. Lu†**
The University of Illinois at Chicago
Chicago, Illinois 60680

D.P. Townsend‡
National Aeronautics and Space Administration
Cleveland, Ohio 44135

and

M. Hawkins§
Allison Engine Company
Indianapolis, IN 46206

ABSTRACT

An approach is proposed for computerized simulation of meshing of aligned and misaligned involute helical gears. Algorithms for TCA (Tooth Contact Analysis) computer programs were developed. Influence of misalignment on the shift of the bearing contact and transmission errors has been investigated. Numerical examples that illustrate the developed theory are provided.

NOMENCLATURE

α_c	parabola coefficient of function that represents the tooth profile of pinion rack-cutter (Fig. 10)
H_i	lead
m_{21}	gear ratio
M_{ij}	coordinate transformation matrix (from S_j to S_i)
$n_f^{(i)}$ $(i = 1,2)$	unit normal vector to surface Σ_i represented in coordinate system S_f
$n_i(\theta_i)$ $(i = 1, 2)$	unit normal to surface Σ_i
N_i	tooth number of the pinion $(i = 1)$ or the gear $(i = 2)$
N_r	normal vector to the rack-cutter surface Σ_r $(r = c,t)$
p_i $(i = 1,2)$	screw parameter
p_{ti} $(i = 1,2)$	circular pitch in transverse section
P_n	normal diametral pitch

*Dr., Professor, ASME Fellow.
†Dr., ASME Member.
‡ASME Fellow.
§ASME Member.

r_{bi} $(i = 1,2)$	radius of base cylinder (Figs. A.1.1 and A.1.2)
r_{pi} $(i = 1,2)$	radius of pitch circle of the pinion (gear)
$\mathbf{r}_f^{(i)}$	position vector of surface Σ_i represented in coordinate system S_f
r_i (u_i, θ_i) $(i = 1,2)$	position vector represented in S_i
s_{t2}	gear tooth thickness on the pitch cylinder
S_i	coordinate system i
u_r, l_r $(r = c,t)$	Surface parameters of Σ_r (Figs. 10 and A.5.1)
$v^{(ij)}$	Relative velocity of surface Σ_i point with respect to surface Σ_j point
w_{t1}	Pinion space width on the pitch cylinder
α_{ti}	Profile angle of the involute profile at the point of intersection of the involute profile with the pitch circle (Figs. A.1.1 and A.1.2)
β	helix angle on the pinion (gear) pitch cylinder (Figs. 9 and A.5.1)
θ_i, u_i $(i = 1,2)$	surface parameters (see θ_i in Figs. A.1.1 and A.1.2)
μ_1	half of angular width on base cylinder (Fig. A.1.1)
$\Delta\alpha_{n1}$	error of profile angle of normal section of pinion rack-cutter
Δ_γ	error of shaft angle (Fig. A.1.3)
$\Delta\lambda_{p1}$	error of pinion lead angle λ_{p1}
$\Delta\phi_2$	gear transmission error (Fig. 3)
η_2	half of tooth thickness on base cylinder (Fig. A.1.2)
λ_{bi} $(i = 1,2)$	lead angle on the base cylinder of radius r_{bi}
λ_{pi} $(i = 1,2)$	lead angle on the pitch cylinder of radius r_{pi}
Σ_i $(i = 1,2)$	pinion and gear tooth surfaces
Σ_r $(r = c,t)$	rack-cutter surfaces
ψ_i $(i = 1,2)$	rotation angles of pinion and gear being in mesh with the rack-cutter Σ_r $(r = c,t)$, respectively (Fig. A.5.2)

1. INTRODUCTION

Computerized simulation of meshing and contact (Tooth Contact Analysis - TCA) was developed for spiral bevel and hypoid gear drives with tooth surfaces are in point contact, (User's Manual, Litvin, F.L. and Gutman, Y., 1981, Litvin, F.L., et al., 1995, and Stadtfeld, H.J., 1993.) There is a great need to develop TCA computer programs for tooth surfaces that are initially in line contact that become point contact due to misalignment. A typical example of such gear drives is the conventional involute helical gear drive.

An approach is proposed that permits the investigation of the influence of gear misalignment on the shift of the bearing contact and transmission errors. Effective methods of crowning of gear tooth surfaces are proposed. The approach is complemented with a TCA computer program. Numerical examples that illustrate the developed approach are provided.

2. SIMULATION OF MESHING

General Considerations

For simulation of meshing, coordinate systems S_1 and S_2 that are rigidly connected to pinion 1 and gear 2, respectively (Fig. A.1.3), are applied. The meshing, of the gear tooth surfaces is considered in the fixed coordinate system S_f that is rigidly connected to the housing. Coordinate system S_p is an auxiliary fixed coordinate system. Coordinate system S_q is applied to simulate misalignment (Fig. A.1.3). Gear tooth surface Σ_i (i = 1,2) of a helical gear and the surface unit normal are represented in S_i by vector functions $\mathbf{r}_i(u_i, \theta_1)$ and $\mathbf{n}_i(\theta_1)$, respectively, where (u_i, θ_1) are the surface parameters (see Appendix 1). Using coordinate transformation from S_i to S_f, we represent the conditions of continuous tangency of gear tooth surfaces by following vector Eqs.(2-5).

$$\mathbf{r}_f^{(1)}(u_1, \theta_1, \phi_1) - \mathbf{r}_f^{(2)}(u_2, \theta_2, \phi_2) = 0 \qquad (1)$$

$$\mathbf{n}_f^{(1)}(\theta_1, \phi_1) - \mathbf{n}_f^{(2)}(\theta_2, \phi_2) = 0 \qquad (2)$$

Vector Eqs. (1) and (2) yield only five independent equations

$$f_i(u_1\theta_1, \phi_1, u_2, \theta_2, \phi_2) = 0 \quad f_i \in C^1 \ (i = 1,2,\ldots,5) \quad (3)$$

since

$$\left|\mathbf{n}_f^{(1)}\right| = \left|\mathbf{n}_f^{(2)}\right| = 1 \qquad (4)$$

Equation system (3) contains six unknowns but one parameter, say ϕ_1, may be chosen as input. The continuous solution of equation system (3) is an iterative process that is based on the following considerations:

(1) Assume that system (3) of nonlinear equations is satisfied at a point

$$P^{(0)} = \left(u_1^{(0)}, \theta_1^{(0)}, \phi_1^{(0)}, u_2^{(0)}, \theta_2^{(0)}, \phi_2^{(0)}\right) \qquad (5)$$

and the Jacobian of the fifth order satisfies the requirement

$$\Delta_5 = \left|\frac{\partial f_i}{\partial u_1}\frac{\partial f_i}{\partial \theta_1}\frac{\partial f_i}{\partial u_2}\frac{\partial f_i}{\partial \theta_2}\frac{\partial f_i}{\partial \phi_2}\right| \neq 0 \quad \left(i = \overline{1,5}\right) \qquad (6)$$

(2) Then we can solve Eqs. (3) in the neighborhood of $P^{(0)}$ by functions

$$\left\{u_1(\phi_1), \theta_1(\phi_1), u_2(\phi_1), \theta_2(\phi_1), \phi_2(\phi_1)\right\} \in C^1 \qquad (7)$$

(3) Inequality (6) is observed when the gear tooth surfaces are in point contact. In this case, using functions (7) we are able to obtain: (*i*) the path of contact on surface Σ_i (i = 1,2) represented as

$$\mathbf{r}_i(u_i, \theta_i), u_i(\phi_i), \theta_i(\phi_i) \qquad (8)$$

and (*ii*) the transmission errors determined as

$$\Delta\phi_2(\phi_1) = \phi_2(\phi_1) - \frac{N_1}{N_2}\phi_1 \qquad (9)$$

The solution discussed above is found numerically. A subroutine for solution of nonlinear equations is represented in User's Manual, 1989. The approach discussed is applied for simulation of meshing of misaligned helical gears. As a reminder that due to misalignment the line contact of tooth surfaces is turned out into point contact.

Edge Contact

Equations (1) and (2) describe continuous surface-to-surface tangency. However, it is not excluded that due to misalignment edge contact will occur that means curve-to-surface tangency when the edge of a surface of one gear (represented as a curve) will contact the surface of the mating gear. Considering the case when the edge of the pinion is in mesh with the surface of the gear, we will use the following equations

$$\mathbf{r}_f^{(1)}\left(u_1(\theta_1), \theta_1, \phi_1\right) = \mathbf{r}_f^{(2)}\left(u_2\ \theta_2, \phi_2\right) \qquad (10)$$

$$\frac{\partial \mathbf{r}_f^{(1)}}{\partial \theta_1} \cdot \mathbf{n}_f^{(2)} = 0 \qquad (11)$$

Equations (10) and (11) represent a system of four nonlinear equations in four unknowns (f_1 is considered as the input paramter). The solution to the system of Eqs. (10) and (11) allow to obtain functions

$$\theta_1(\phi_1),\ \theta_2(\phi_1), u_2(\phi_1), \phi_2(\phi_1) \qquad (12)$$

All three cases of meshing, such as surface-to-surface with instantaneous point contact, edge contact, and line contact (see below), may exist in meshing of involute helical gears when they are misaligned or aligned.

Simulation of Meshing of Aligned Helical Gears

In this case, the gear tooth surfaces are in line ctonact and the Jacobian D_5 (Eq. (6)) becomes equal to zero. The TCA is based on the algorithm represented in Appendix 3. Two input parameters, say f_1 and u_1, must be applied and then we will get that the matrix

$$\left|\frac{\partial f_i}{\partial \theta_1}\ \frac{\partial f_i}{\partial u_2}\ \frac{\partial f_i}{\partial \theta_2}\ \frac{\partial f_i}{\partial \phi_2}\right| \quad \left(i = \overline{1,4}\right) \qquad (13)$$

will be of rank 4. THe instantaneous line of contact on surface $\sum_i (i=1,2)$ is the q—line of the vector function $\mathbf{r}_i(u_i, q_i)$. This line is the tangent to the helix on the base cylinder of gear i (Fig. 1). Computations confirm that the transmission funciton is a linear one represented as

$$\phi_2(\phi_1) = \frac{N_1}{N_2}\phi_1 \qquad (14)$$

and the transmission errors are zero.

Simulation of Meshing of Misaligned Involute Helical Gears

The TCA computer program developed was applied to investigate of the following erros: Dg—the shaft angle error (when the axes become crossed), Da_{n1} normal proifle angle error of the rack-cutter that generates the pinion, and Dl_{p1}—pinion lead angle error on the pitch cylinder.

The manufacturing of helical gears is based on application of two imaginary rack-cutters that like a molding complements a casting. The pinion and the gear are generated separately, but the imaginary rack-cutters have the same profile angle a_n in the normal section. Error Da_{n1} means that $a_{n1} \neq a_{n2}$.

Parameter a_n does not exist directly in the surface and surface unit normal equations (see Appendix 1). However, error Da_{n1} affects the design parameters a_{t1}, r_{b1}, and l_{b1} as follows (see Appendix 2)

$$\Delta\alpha_{t1} = \frac{\sin 2\alpha_{t1}}{\sin 2\alpha_{n1}}\Delta\alpha_{n1} \qquad (15)$$

$$\Delta\lambda_{b1} = \frac{\sin 2\lambda_{b1} \tan\alpha_{t1}}{2}\Delta\alpha_{t1} \qquad (16)$$

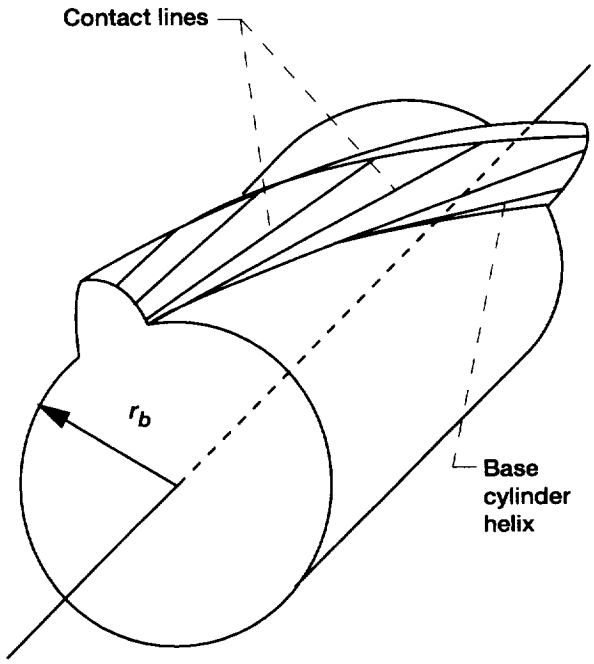

Figure 1.—Contact lines on tooth surfaces of a helical gear.

$$\Delta r_{b1} = -r_{p1} \sin \alpha_{t1} \Delta \alpha_{t1} \tag{17}$$

In the real process of manufacturing, error Dl_{p1} is caused due to lead error H_1. Using the relationships between the design parameters (see Appendix 2), the following is obtained:

$$\Delta \lambda_{p1} = \frac{\sin 2\lambda_{p1}}{2H_1} \Delta H_1 \tag{18}$$

Equation (18) permits Dl_{p1} to be obtained considering the lead error DH_1 is known.

Due to misalignment, the line contact of tooth surfaces is turned into point contact. The TCA for point contact is based on the application of equation system (3). The algorithm for initial guess for the solution of equation system (3) is represented in Appendix 4.

The influence of errors Dg, Da_{n1}, and Dl_{p1} was investigated in the following ways: (i) as the impact by the separate action of each of the errors, and (ii) as the impact by action of the following combination of errors: Dg, Dl_{p1}, and Da_{n1} and Dl_{p1}.

The separate action of errors Dl and Dl_{p1} causes an edge contact (Fig. 2) and a discontinuous, almost linear function of transmission errors (Fig. 3). Error Da_{n1} causes paths of contact shown in Fig. 4 but does not cause transmission errors. The drawings shown in Figs. 2 to 4 are based on computation for a gear drive with the following data: $N_1 = 30$, $N_2 = 100$, $a_n = 20°$, $P_n = 5$(1/in.), $l_p = 60°$, and $L = 1.6$(in.).

The combination of errors Dg and Dl_{p1} when $|\Delta\gamma| \neq |\Delta\lambda_{p1}|$ causes also an edge contact (Fig. 5). The function of transmission errors for one cycle of meshing is a combination of two almost linear functions with different values of slope (Fig. 6). The combination of errors Da_{n1} and Dl_{p1} causes the path of contact on the edge of the tooth length (Fig. 7) and an almost linear function of transmission errors (Fig. 8).

There is a particular case, when $|\Delta\gamma| \neq |\Delta\lambda_{p1}|$. The meshing of gears may be considered in such a case as meshing of crossed involute helical gears which tooth surfaces are in point contact. The path of contact on the tooth surface is shown in Fig. 9, the transmission function is a linear one, and there is no transmission errors. However, the meshing of gear is not stable because even a small difference between $|\Delta\gamma| \neq |\Delta\lambda_{p1}|$ will cause an edge contact and transmission errors.

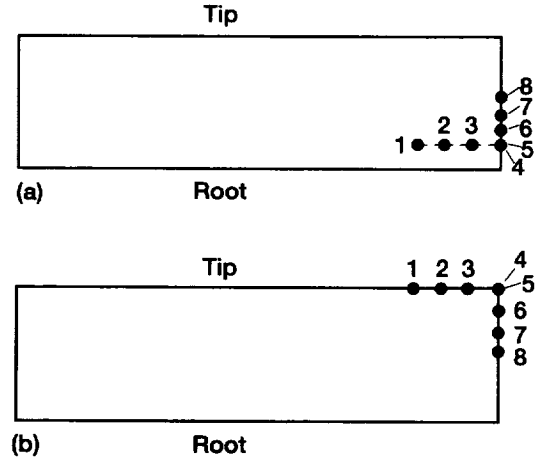

Figure 2.—Edge contact caused by $\Delta\gamma$ or $\Delta\lambda_p$l = 3 arc min: (a) pinion tooth surface, (b) gear tooth surface.

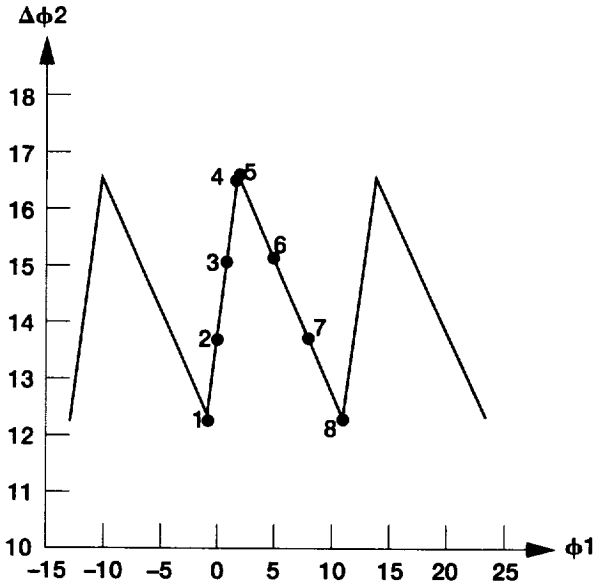

Figure 3.—Function of transmission errors caused by $\Delta\gamma$ or $\Delta\lambda_p$l = 3 arc min.

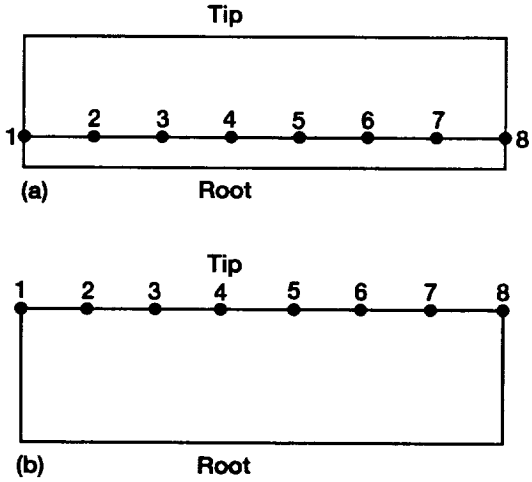

Figure 4.—Path of contact caused by $\Delta\alpha$nl = 3 arc min: (a) pinion tooth surface, (b) gear tooth surface.

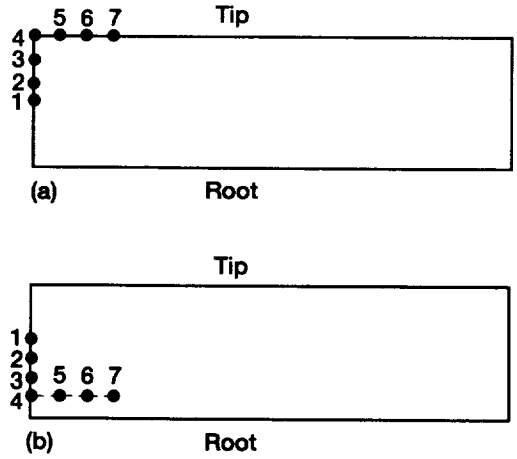

Figure 5.—Edge contact caused by $\Delta\gamma$ = 3 arc min and $\Delta\lambda_p$l = −4 arc min: (a) pinion tooth surface, (b) gear tooth surface.

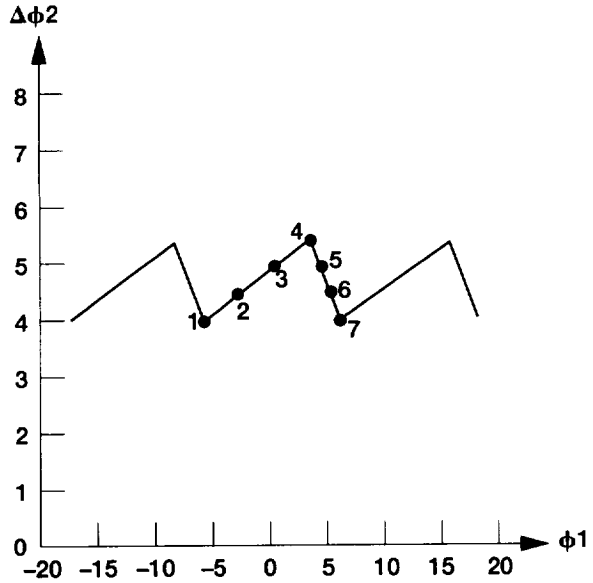

Figure 6.—Function of transmission errors caused by $\Delta\gamma$ = 3 arc min and $\Delta\lambda_p$l = –4 arc min.

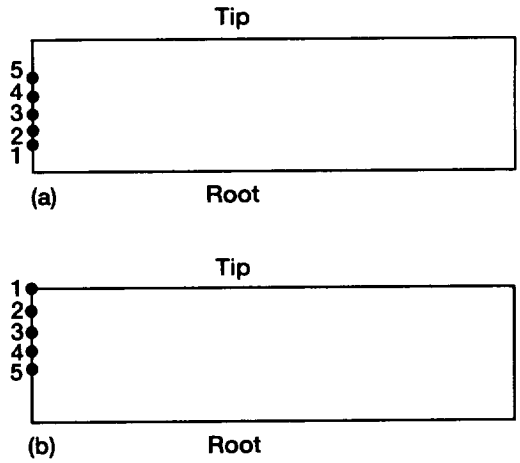

Figure 7.—Edge contact caused by $\Delta\alpha$n1 = 3 arc min and $\Delta\lambda_p$l = –2 arc min: (a) pinion tooth surface, (b) gear tooth surface.

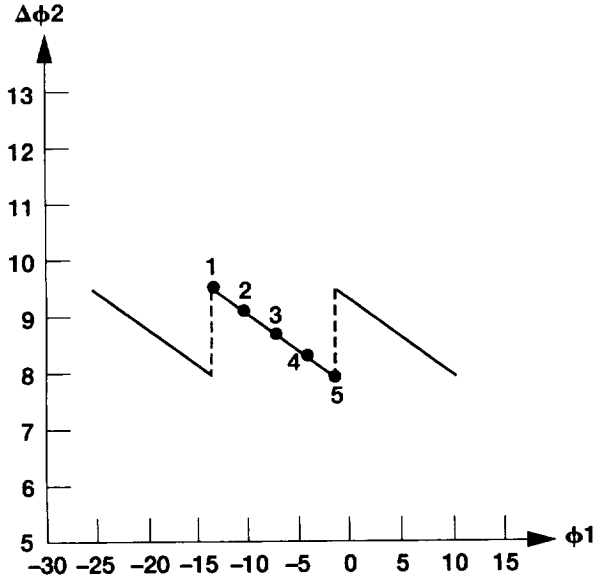

Figure 8.—Function of transmission errors caused by $\Delta\alpha$n1 = 3 arc min and $\Delta\lambda_p$l = –2 arc min.

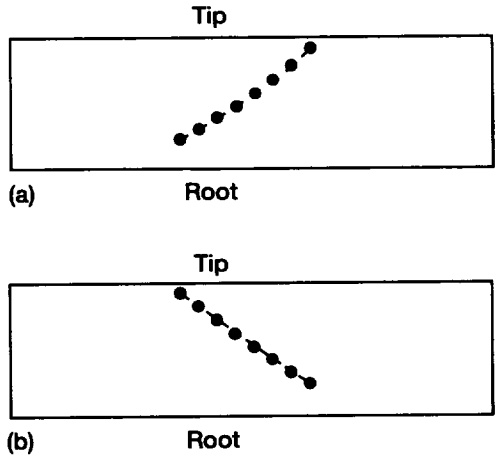

Figure 9.—Path of contact caused by $\Delta\gamma$ = 3 arc min and $\Delta\lambda_p$l = –3 arc min: (a) pinion tooth surface, (b) gear tooth surface.

3. GENERATION AND MODIFICATION OF TOOTH SURFACES

The derivation of tooth surfaces is based on the imaginary process of generation of conjugate surfaces by application of two rack-cutters. The generating surfaces of the rack-cutters are represented respectively by plane Σ_t and cylindrical surface Σ_c that differs slightly from plane Σ_t (Fig. 10). The rack-cutter surfaces Σ_c and Σ_t are rigidly connected each to other in the process of the imaginary generation, and they are in tangency along straight line $o_b z_b$ (Fig. 10). This line and axes of the gears form angle b, that is equal to the helix angle on the pinion (gear) pitch cylinder. Figure 11 shows the normal sections of the rack-cutters. Rack-cutter surface Σ_c generates the pinion tooth surface Σ_1, and a rack-cutter surface Σ_t generates the gear tooth surface Σ_2.

Applied Coordinate Systems

Movable coordinate systems S_r ($r = c,t$), S_1 and S_2 are rigidly connected to the tools (rack-cutters), the pinion and the gear, respectively. The fixed coordinate systems S_m and S_n are rigidly connected to the frame of the cutting machine (Fig. A.5.2).

Generating Surface

The rack-cutter surface Σ_t ($r = c,t$) is represented in S_r by the equation

$$\mathbf{r}_r = \mathbf{r}_r(u_r, l_r) \tag{19}$$

where u_r, l_r are the surface parameters.

The normal to the rack-cutter surface is represented as

$$\mathbf{N}_r = \frac{\partial \mathbf{r}_r}{\partial l_r} \times \frac{\partial \mathbf{r}_r}{\partial u_r} \tag{20}$$

Equations (19) and (20) must be derived twice to represent the working surfaces of two rack-cutters that generate the pinion and the gear, respectively (see Appendix 5).

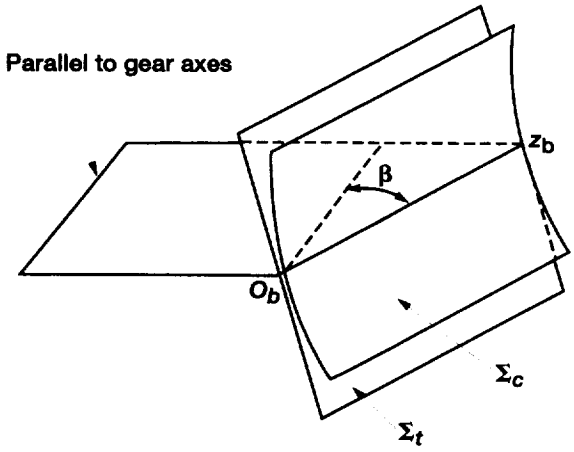

Figure 10.—Rack-cutter surfaces.

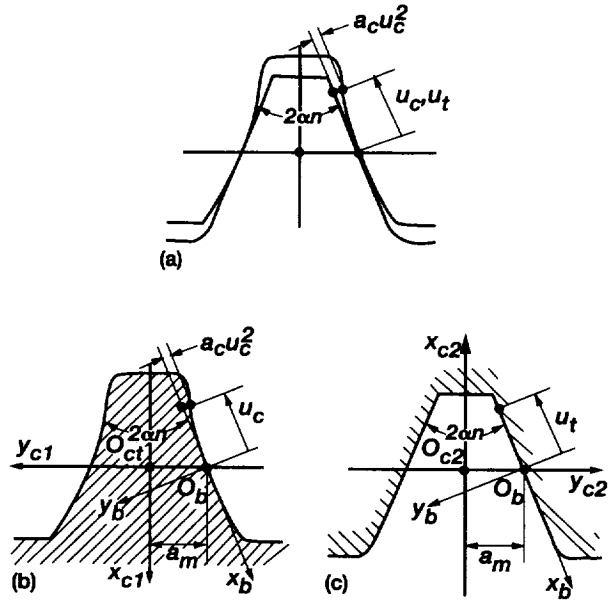

Figure 11.—Normal sections of rack-cutters.

Generated Surface

The generated surface Σ_i. (i = 1,2), the pinion or the gear surface, is determined as the envelope to the family of rack-cutter surfaces. Surface Σ_i is determined in S_i (see Appendix 5) by the Eqs. (3) and (4).

$$\mathbf{r}_i(u_r, l_r, \psi_i) = \mathbf{M}_{ir}(\psi_i)\mathbf{r}_i(u_r, l_r) \qquad (21)$$

$$\mathbf{N}_r \cdot \mathbf{v}_r^{(ri)} = f(u_r, l_r, \psi_i) = 0 \qquad (22)$$

Here: (u_r, l_r) are the rack-cutter surface parameters; y_i is the generalized parameter of motion in the process for generation; $\mathbf{N}_r$ is the normal to the rack-cutter surface; $\mathbf{v}_r^{(ri)}$ is the relative velocity in meshing of the rack-cutter and the generated surface. Equation (21) represents in S_i the family of rack-cutter surfaces. Equation (22) is the equation of meshing that is the necessary condition of envelope existence.

Equations (21) and (22) represent surface Σ_i by three related parameters. Taking into account that l_r is a linear parameter in equation of meshing, it can be eliminated and surface Σ_i can be represented in two-parameter form, by parameters u_r, y_i (see Appendix 5).

Simulation of Meshing

Using the conditions of continuous tangency of gear tooth surfaces (1) and (2), and solving the equation systems (3), we can obtain the contact path on pinion and gear tooth surfaces, respectively. Since the pinion tooth surface is modified and generated by cylindrical surface Σ_c of the rack-cutter, the pinion and gear tooth surfaces are in mesh in point contact. The contact path is directed along the tooth length. Although the misalignment Dg occurs, the contact path is still close to the mean line. Figures 12 and 13 show the TCA results for the case of Dg = 3 arc min. Figure 12 shows that the contact path is in the middle of the pinion (gear) tooth surface and Fig. 13 shows that the function of transmission errors is an almost linear. The results of TCA confirm that the localization of contact is a necessary but not a sufficient condition of the improvement of meshing of helical gears. Due to the shape of transmission errors shown in Fig. 13, the transfer of meshing to the neighboring pair of teeth will be accompanied with high acceleration and vibration. This defect can be avoided by application of a predesigned parabolic function of transmission errors that is able to absorb the almost linear function of transmission errors (Litvin, F.L., 1994). Various methods of the predesign of a parabolic function of transmission errors were proposed in Litvin, F.L., et al., 1995.

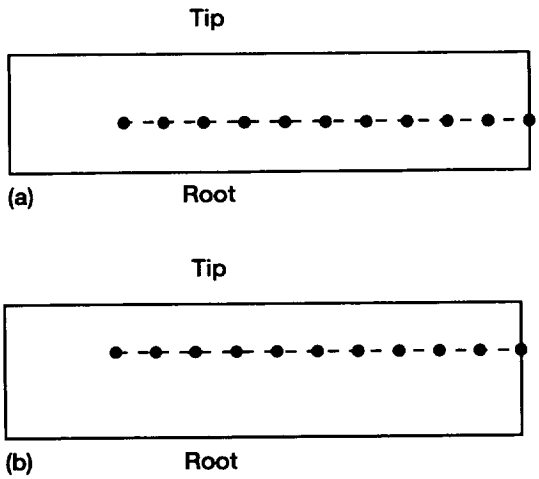

Figure 12.—Path of contact caused by Δγ = 3 arc min: (a) modified pinion tooth surface, (b) gear tooth surface.

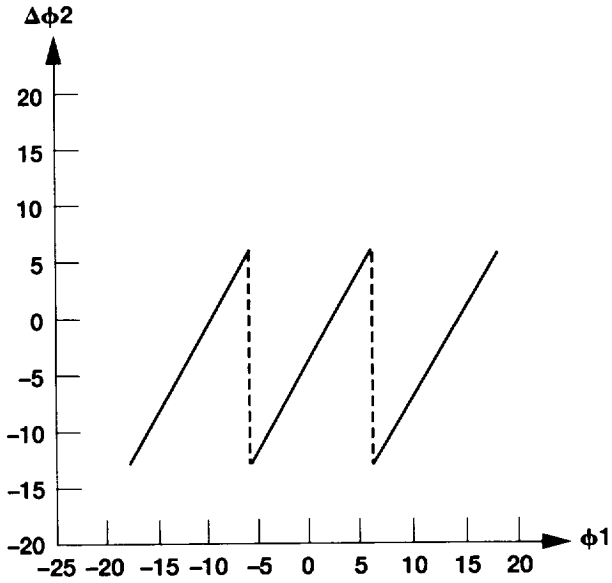

Figure 13.—Function of transmission errors for modified involute helical gear drive when Δγ = 3 arc min.

4. CONCLUSION

Based on the study contained herein the following conclusions can be drawn:

1. Equations of gear tooth surfaces with localized bearing contact were developed.
2. Algorithms for TCA (Tooth Contact Analysis) of aligned and misaligned involute helical gear drives have been developed.
3. Numerical examples that illustrate the developed theory and permit one to determine the influence of errors of alignment are presented. Lead correction may be accompanied with edge contact (Fig. 2).

REFERENCES

1. IMSL MATH/LIBRARY: User's Manual, MALB-USM-UNBND-EN 8901–1.1, 2500, Citywest B1., Houston, Texas 77042–3020, 1989.
2. Litvin, F.L. and Gutman, Y.: "Methods of Synthesis and Analysis for Hypoid Gear-Drives of Formate and Helixform," *Journal of Mechanical Design*, 103: 83–113, 1981.
3. Litvin, F.L.: *Theory of Gearing* (in Russian), 1st ed. in 1960, 2nd ed. in 1968.
4. Litvin, F.L.: *Gear Geometry and Applied Theory,* Prentice Hall, Englewood Cliffs, NJ, 1994.
5. Litvin, F.L. et al.: "Computerized Design and Generation of Low-Noise Helical Gears with Modified Surface Topology," *Journal of Mechanical Design*, 117: 254–261, 1995.
6. Stadtfeld, H.J: *Handbook of Bevel and Hypoid Gear*, Rochester Institute of Technology, 1993.

APPENDIX 1. EQUATIONS OF PINION AND GEAR TOOTH SURFACES

The equations presented in Litvin, F.L., 1994 for tooth surfaces of helical involute gears and the coordinate systems are used. The tooth side surface II (Σ_1) of a left-hand pinion (see the cross-section in Fig. A.1.10) and the unit normal $\mathbf{n}_1$ to the surface are represented as follows:

$$\mathbf{r}_1(u_1, \theta_1) = \begin{bmatrix} r_{b1}\cos(\theta_1 + \mu_1) + u_1 \cos\lambda_{b1} \sin(\theta_1 + \mu_1) \\ -r_{b1}\sin(\theta_1 + \mu_1) + u_1 \cos\lambda_{b1} \cos(\theta_1 + \mu_1) \\ -u_1 \sin\lambda_{b1} + p_1\theta_1 \end{bmatrix} \quad \text{(A.1.1)}$$

$$\mathbf{n}_1(q_1) = \begin{bmatrix} -\sin\lambda_{b1}\sin(q_1 + m_1) \\ -\sin\lambda_{b1}\cos(q_1 + m_1) \\ -\cos\lambda_{b1} \end{bmatrix} \quad \text{(A.1.2)}$$

The surface tooth side II (Σ_2) of a right-had gear (see the cross-section in Fig. A.1.2) and the unit normal $\mathbf{n}_2$ to the surface are represented by the equations

$$\mathbf{r}_2(u_2, \theta_2) = \begin{bmatrix} r_{b2}\cos(\theta_2 - \eta_2) + u_2 \cos\lambda_{b2} \sin(\theta_2 - \eta_2) \\ -r_{b2}\sin(\theta_2 - \eta_2) + u_2 \cos\lambda_{b2} \cos(\theta_2 - \eta_2) \\ u_2 \sin\lambda_{b2} - p_2\theta_2 \end{bmatrix} \quad \text{(A.1.3)}$$

$$\mathbf{n}_2(\theta_2) = \begin{bmatrix} \sin\lambda_{b2}\sin(\theta_2 - \eta_2) \\ \sin\lambda_{b2}\cos(\theta_2 - \eta_2) \\ -\cos\lambda_{b2} \end{bmatrix} \quad \text{(A.1.4)}$$

Here: (u_i, q_i) $(i = 1,2)$ are the surface parameters. The relationships between the design parameters are represented in Appendix 2 and their notations are given in the nomenclature.

For simulation of meshing coordinate systems S_1 and S_2 that are rigidly connected to pinion 1 and gear 2, respectively (Fig. A.1.3) are applied. The meshing of the gear tooth surfaces is considered in the fixed coordinate system S_f that is rigidly connected to the housing. Coordinate system S_p is an auxiliary fixed coordinate system. Coordinate system S_q is applied to simulate the errors of assembly (Fig. A.1.3).

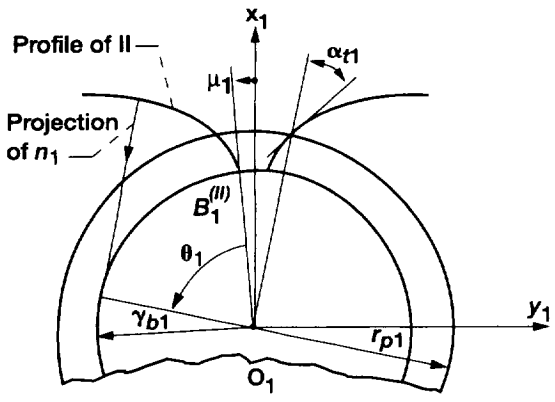

Figure A.1.1.—Cross section of helical pinion (1).

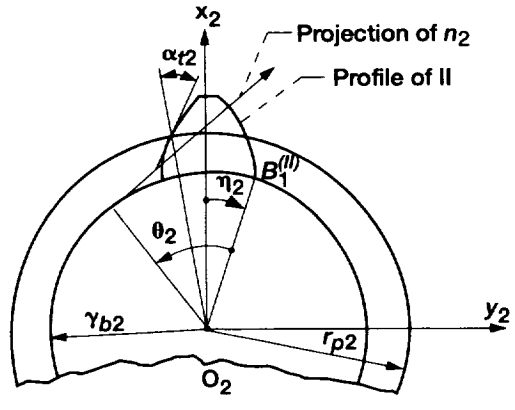

Figure A.1.2.—Cross section of helical gear (2).

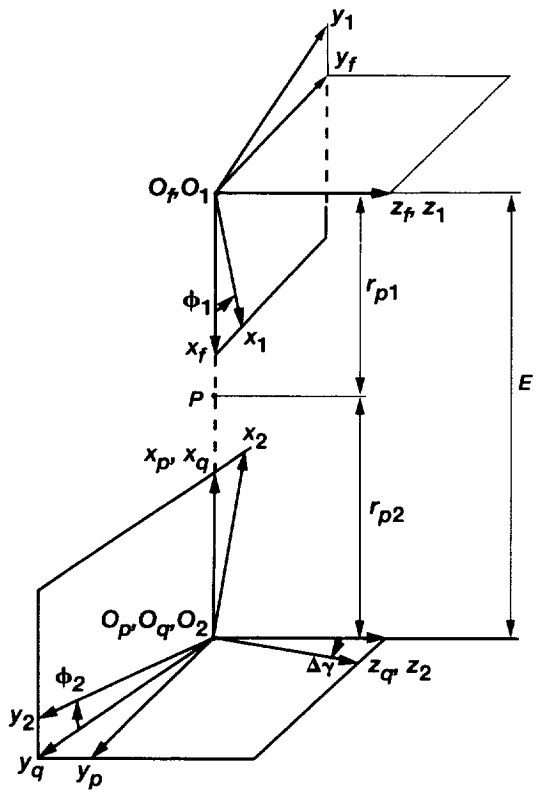

Figure A.1.3.—Applied coordinate system.

APPENDIX 2.—RELATIONS BETWEEN THE DESIGN PARAMETERS

The input design parameters are : N_1, N_2, P_n, α_n, and λ_p. For ideal gearing we have: $\alpha_{n1} = \alpha_{n2}$, $\lambda_{p1} = \lambda_{p2}$, $\lambda_{b1} = \lambda_{b2}$. The remaining design parameters (see the nomenclature) are determined as follows

$$\tan \alpha_{ti} = \frac{\tan \alpha_{ni}}{\sin \lambda_{pi}}, (i = 1,2) \qquad \text{(A.2.1)}$$

$$p_{ti} = \frac{\pi}{P_n \sin \lambda_{pi}} \qquad \text{(A.2.2)}$$

$w_{t1} = \frac{P_n}{2}$ (assuming that the backlash is zero) (A.2.3)

$$s_{t2} = \frac{P_{t2}}{2} \qquad \text{(A.2.4)}$$

$$r_{pi} = \frac{N_i}{2P_n \sin \lambda_{pi}} \qquad \text{(A.2.5)}$$

$$r_{bi} = r_{pi} \cos \alpha_{ti} \qquad \text{(A.2.6)}$$

$$\tan \lambda_{bi} = \frac{\tan \lambda_{pi}}{\cos \alpha_{ti}} \qquad \text{(A.2.7)}$$

$$p_i = r_{bi} \tan \lambda_{bi} = r_{pi} \tan \lambda_{pi} \qquad \text{(A.2.8)}$$

$$H_i = 2\pi_{pi} \qquad \text{(A.2.9)}$$

$$\frac{p_1}{p_2} = \frac{r_{b1}}{r_{b2}} = \frac{r_{p1}}{r_{p2}} = \frac{N_1}{N_2} = m_{21} \qquad \text{(A.2.10)}$$

APPENNDIX 3.—ALGORITHM OF TCA FOR ALIGNED GEARS

The TCA computer program requires the solution of the system of Eq. (3). The algorithm developed is based on computation by the following steps:

Step 1: In the case of aligned gears we have

$$\lambda_{b1} = \lambda_{b2} = \lambda_b \tag{A.3.1}$$

Step 2: Considering $n_{xf}^{(1)} = n_{xf}^{(2)}$ and $n_{yf}^{(1)} = n_{yf}^{(2)}$, we obtain the equation

$$\theta_1 + \mu_1 - \phi_1 = \theta_2 - \eta_2 + \phi_2 \tag{A.3.2}$$

where f_1 is the input parameter.

Step 3: Considering $x_f^{(1)} = x_f^{(2)}$ and Eqs. (A.3.1) to (A.3.2), we obtain

$$\begin{aligned}(r_{b1} + r_{b2})\cos(\theta_1 + \mu_1 - \phi_1) + (u_1 + u_2) \\ \times \cos\lambda_b \sin(\theta_1 + \mu_1 - \phi_1) = \mathrm{E}\end{aligned} \tag{A.3.3}$$

Step 4: Considering $y_f^{(1)} = y_f^{(2)}$ and Eqs. (A.3.1) to (A.3.2), we obtain

$$\begin{aligned}(r_{b1} + r_{b2})\sin(\theta_1 + \mu_1 - \phi_1) + (u_1 + u_2) \\ \times \cos\lambda_b \cos(\theta_1 + \mu_1 - \phi_1) = 0\end{aligned} \tag{A.3.4}$$

Step 5: Considering $z_f^{(1)} = z_f^{(2)}$ and Eq. (A.3.1), we obtain

$$(u_1 + u_2)\sin\lambda_b - p_1\theta_1 - p_2\theta_2 = 0 \tag{A.3.5}$$

Step 6: Equations (A.3.3) and (A.3.4) yield

$$\theta_1 = \alpha_t + \phi_1 - \mu_1 \tag{A.3.6}$$

Step 7: Equations (A.3.4) and (A.3.5) yield

$$\theta_2 = \left(\frac{N_1}{N_2} + 1\right)\tan\alpha_t - \frac{N_1}{N_2}\theta_1 \tag{A.3.7}$$

Step 8: Equations (A.3.2) and (A.3.6) yield

$$\phi_2 = \eta_2 - \theta_2 + \alpha_t \tag{A.3.8}$$

Step 9: Equation (A.3.5) yields

$$u_2 = \frac{r_{b1}\theta_1 + r_{b2}\theta_2}{\cos\lambda_b} - u_1 \tag{A.3.9}$$

Note: parameter u_1 is the second input parameter, in addition to ϕ_1, that is required for the TCA for aligned gears.

APPENDIX 4.—TCA ALGORITHM FOR MISALIGNED GEAR DRIVES

An initial guess is required for the solution of equation system (3) in the case of gear misalignment. The required set of parameters, $P^{(0)} = \left(u_1^{(0)}, \theta_1^{(0)}, \phi_1^{(0)}, u_2^{(0)}, \theta_2^{(0)}, \phi_2^{(0)}\right)$, can be obtained by the following derivations

Step 1: Using equation $n_{zf}^{(1)} = n_{zf}^{(2)}$, we obtain

$$\cos\Phi_2 = \frac{\cos\lambda_{b1} - \cos\lambda_{b2}\cos\Delta\gamma}{\sin\lambda_{b2}\sin\Delta\gamma}, \quad (\Phi_2 = \theta_2 - \eta_2 + \phi_2) \tag{A.4.1}$$

We consider that when pinion lead angle error, Dl_{p1}, occurs, we have $\lambda_{b1} \neq \lambda_{b2}$ and $\lambda_{p1} \neq \lambda_{p2}$ (see Appendix 2).

Step 2: Using equation $n^{(1)}{}_{xf} = n^{(2)}{}_{xf}$, we obtain

$$\sin\Phi_1 = \frac{\sin\lambda_{b2}}{\sin\lambda_{b1}}\sin\Phi_2, \ (\Phi_1 = \theta_1 + \mu_1 - \phi_1) \tag{A.4.2}$$

Step 3: Using equation $x_f^{(1)} = x_f^{(2)}$, we obtain

$$u_2 = \frac{1}{\cos\lambda_{b2}\sin\Phi_2}\left(E - r_{b2}\cos\Phi_2 - x_f^{(1)}\right) \tag{A.4.3}$$

Step 4: Using equation $y_f^{(1)} = y_f^{(2)}$, we obtain

$$\theta_2 = \frac{1}{p_2\sin\Delta\gamma}\left[y_f^{(1)} + u_2\sin\lambda_{b2}\sin\Delta\gamma - \left(r_{b2}\sin\Phi_2 - u_2\cos\lambda_{b2}\cos\Phi_2\right)\cos\Delta\gamma\right] \tag{A.4.4}$$

Step 5: Using equaton $z_f^{(1)} = z_f^{(2)}$, we obtain

$$\theta_1 = \frac{1}{p_1}\left(z_f^{(2)} + u_1\sin\lambda_{b1}\right) \tag{A.4.5}$$

Step 6: Equation (A.4.2) yields

$$\phi_1 = \theta_1 + \mu_1 - \Phi_1 \tag{A.4.6}$$

Step 7: Equations (A.4.1) and (A.4.2) yield

$$\phi_2 = \Phi_2 - \theta_2 + \eta_2 \tag{A.4.7}$$

When u_1 is chosen, the other five parameters may be determined by Eqs. (A.4.3) to (A.4.7). Parameter u_1 is related with the magnitude r_1 of the position vector of the pinion cross-section by the equation

$$u_1 = \frac{\sqrt{r_1^2 - r_{b1}^2}}{\cos \lambda_{b1}} \qquad \text{(A.4.8)}$$

where $r_{d1} \leq r_1 \leq r_{a1}$.

Equations (A.4.3) to (A.4.5) and (A.4.7) to (A.4.8) permit one to determine parameters $P^{(0)}$ as the initial guess for the solution of the system of Eq. (3) considering that f_1 is given.

APPENDIX 5.—SURFACES OF TOOTH RACK-CUTTERS

As a reminder, that two rack-cutters are applied for the separate generation of the gear and the pinion (Fig. 11(a)). The gear rack-cutter is a conventional one that is used for generation of involute gears and its normal section is represented in S_{c2} (Fig. 11(c)) as

$$r_{c2}(u_t) = \mathrm{M}_{c2b} r_b(u_t) = \begin{bmatrix} u_t \cos\alpha_n \\ a_m - u_t \sin\alpha_n \\ 0 \\ 1 \end{bmatrix} \tag{A.5.1}$$

where (Fig. 11(c))

$$a_m = \frac{\pi}{4P_n}, \mathbf{r}_b(u_b) = \begin{bmatrix} -u_t & 0 & 0 & 1 \end{bmatrix}^T \tag{A.5.2}$$

The equations of the surface and the unit normal to the surface of gear rack-cutter Σ_t are represented in S_t as

$$\mathbf{r}_t(u_t, l_t) = \mathbf{M}_{tc2}\mathbf{r}_{c2}(u_t) \tag{A.5.3}$$

$$\mathbf{n}_t = \frac{\dfrac{\partial \mathbf{r}_t}{\partial l_t} \times \dfrac{\partial \mathbf{r}_t}{\partial u_t}}{\left| \dfrac{\partial \mathbf{r}_t}{\partial l_t} \times \dfrac{\partial \mathbf{r}_t}{\partial u_t} \right|} \tag{A.5.4}$$

where (Fig. A.5.1(b))

$$M_{tc2} = \begin{bmatrix} 1 & 0 & 0 & 0 \\ 0 & \cos\beta & \sin\beta & l_t \sin\beta \\ 0 & -\sin\beta & \cos\beta & l_t \cos\mathrm{n}\beta \\ 0 & 0 & 0 & 1 \end{bmatrix} \tag{A.5.5}$$

For the purpose of localization of contact, the normal section of pinion rack-cutter deviates from the normal section of the gear rack-cutter and is represented in S_{c1} as (Fig. 11(b))

$$\mathbf{r}_{c1}(u_c) = \mathbf{M}_{c1b}\mathbf{r}_b(u_c) = \begin{bmatrix} -u_c \cos\alpha_n - a_c u_c^2 \sin\alpha_n \\ u_c \sin\alpha_n - a_c u_c^2 \cos\alpha_n - \alpha_m \\ 0 \\ 1 \end{bmatrix} \tag{A.5.6}$$

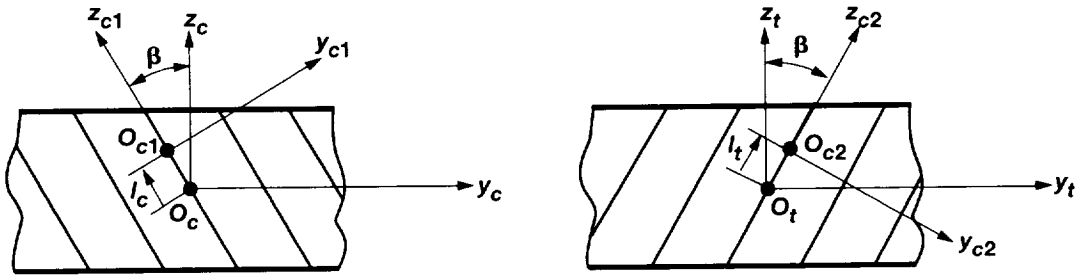

Figure A.5.1.—To derivation of rack-cutter surface.

where

$$\mathbf{r}_b(u_c) = \left[-u_c \;\; -a_c u_c^2 \;\; 0 \;\; 1\right]^T \qquad \text{(A.5.7)}$$

The surface equation of pinion rack-cutter Σ_c is represented in S_c

$$\mathbf{r}_c(u_c, l_c) = \mathbf{M}_{cc1}\mathbf{r}_{c1}(u_c) \qquad \text{(A.5.8)}$$

where (Fig. A.5.1(a))

$$M_{cc1} = \begin{bmatrix} 1 & 0 & 0 & 0 \\ 0 & \cos\beta & -\sin\beta & -l_c\sin\beta \\ 0 & -\sin\beta & \cos\beta & l_c\cos\beta \\ 0 & 0 & 0 & 1 \end{bmatrix} \qquad \text{(A.5.9)}$$

The unit normal to Σ_c is represented in S_c by equations

$$\mathbf{n}_c = \frac{\mathbf{N}_c}{|\mathbf{N}_c|}, \mathbf{N}_c = \frac{\partial \mathbf{r}_c}{\partial l_c} \times \frac{\partial \mathbf{r}_c}{\partial u_c} \qquad \text{(A.5.10)}$$

that yield

$$\mathbf{n}_c = \frac{1}{\sqrt{1+4a_c^2u_c^2}} \begin{bmatrix} -\sin\alpha_n + 2a_c u_c \cos\alpha_n \\ -(\cos\alpha_n + 2a_c u_c \cos\alpha_n)\cos\beta \\ -(\cos\alpha_n + 2a_c u_c \cos\alpha_n)\cos\beta \end{bmatrix} \qquad \text{(A.5.11)}$$

Equation of Meshing

In the process for the generation, the two rigidly connected rack-cutters perform translational motion, while the pinion and gear perform rotational motions as shown in Fig. A.5.2.

The equation of meshing between surface Σ_r ($r = c,t$) of the rack-cutter and the pinion (gear) tooth surface Σ_i ($i = 1,2$) can be represented as

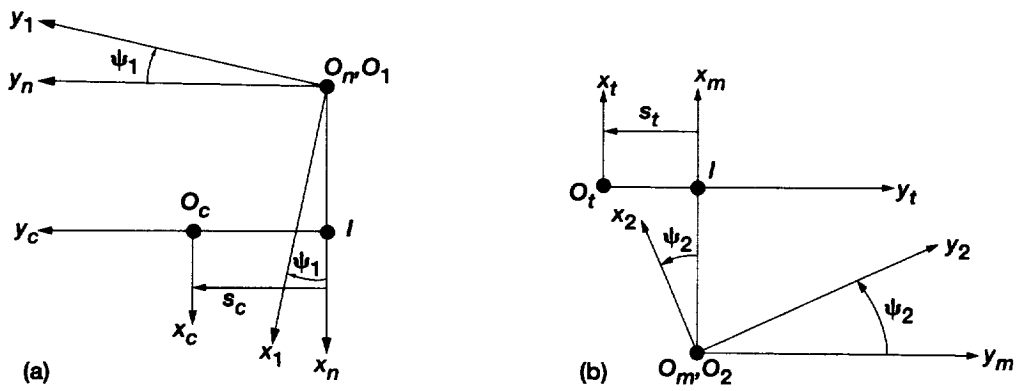

Figure A.5.2.—Generation of pinion and gear by rack-cutters.

$$f(u_r,\ l_r,\ \psi_i) = 0 \qquad \text{(A.5.12)}$$

where y_i is the angle of rotation of the gear in the process for generation. The derivation of equation of meshing is based on the theorem that the common normal to Σ_r and Σ_i must pass through the instantaneous axis of rotaton. Thus, we have

$$\frac{X_r - x_r}{n_{xr}} = \frac{Y_r - y_r}{n_{yr}} = \frac{Z_r - z_r}{n_{zr}} \qquad \text{(A.5.13)}$$

Here (Fig. A.5.2) we have

(i) $(X_t = 0,\ Y_t = r_{p2}y_2)$ in the case for gear generation.

(ii) $(X_c = 0,\ Y_c = -r_{p1}y_1)$ in the case for pinion generation.

After transformations, we obtain the following equations of meshing between Σ_1 and Σ_c, and Σ_2 and Σ_t, respectively

$$f(u_c, l_c, \psi_1) = r_{p1}\psi_1 - l_c \sin\beta - a_m \cos\beta + \frac{u_c\left(1 + 2a_c^2 u_c^2\right)\cos\beta}{\sin\alpha_n - 2a_c u_c \cos\alpha_n} = 0 \qquad \text{(A.5.14)}$$

$$f(u_t, l_c, \psi_2) = r_{p2}\psi_2 - l_t \sin\beta - a_m \cos\beta + \frac{u_t \cos\beta}{\sin\alpha_n} = 0 \qquad \text{(A.5.15)}$$

where ψ_i $(i = 1,2)$ is the angle of pinion and gear rotation.

Tooth Surfaces

Pinion tooth surface Σ_1 is generated by rack-cutter tooth surface Σ_c and is represented in S_1 by the equations

$$\mathbf{r}_1(u_c, l_c, \psi_1) = \mathbf{M}_{1n}\mathbf{M}_{nc}\mathbf{r}_c(u_c, l_c),\ f(u_c, l_c, \psi_1) = 0 \qquad \text{(A.5.16)}$$

where (Fig. A.5.2(a))

$$M_{1n} = \begin{bmatrix} \cos\psi_1 & \sin\psi_1 & 0 & 0 \\ -\sin\psi_1 & \cos\psi_1 & 0 & 0 \\ 0 & 0 & 1 & 0 \\ 0 & 0 & 0 & 1 \end{bmatrix} \qquad \text{(A.5.17)}$$

$$M_{nc} = \begin{bmatrix} 1 & 0 & 0 & r_{p1} \\ 0 & 1 & 0 & r_{p1}\psi_1 \\ 0 & 0 & 1 & 0 \\ 0 & 0 & 0 & 1 \end{bmatrix} \qquad \text{(A.5.18)}$$

Gear tooth surface Σ_2 is represented in S_2 by the following equation

$$\mathbf{r}_2(u_c, l_c, \psi_2) = \mathbf{M}_{2n}\mathbf{M}_{mt}\mathbf{r}_t(u_t, l_t),\ f(u_t, l_t, \psi_2) = 0 \qquad \text{(A.5.19)}$$

where (Fig. A.5.2(b))

$$M_{2m} = \begin{bmatrix} \cos\psi_2 & -\sin\psi_2 & 0 & 0 \\ \sin\psi_2 & \cos\psi_2 & 0 & 0 \\ 0 & 0 & 1 & 0 \\ 0 & 0 & 0 & 1 \end{bmatrix} \qquad \text{(A.5.20)}$$

$$M_{mt} = \begin{bmatrix} 1 & 0 & 0 & r_{p2} \\ 0 & 1 & 0 & -r_{p2}\psi_2 \\ 0 & 0 & 1 & 0 \\ 0 & 0 & 0 & 1 \end{bmatrix} \qquad \text{(A.5.21)}$$

REPORT DOCUMENTATION PAGE

Form Approved
OMB No. 0704-0188

1. AGENCY USE ONLY (*Leave blank*)	2. REPORT DATE	3. REPORT TYPE AND DATES COVERED
	July 1997	Technical Memorandum

4. TITLE AND SUBTITLE

Computerized Simulation of Meshing of Conventional Helical Involute Gears and Modification of Geometry

5. FUNDING NUMBERS

WU–581–30–13
1L162211A47A

6. AUTHOR(S)

F.L. Litvin, J. Lu, D.P. Townsend, and M. Hawkins

7. PERFORMING ORGANIZATION NAME(S) AND ADDRESS(ES)

NASA Lewis Research Center
Cleveland, Ohio 44135–3191
and
U.S. Army Research Laboratory
Cleveland, Ohio 44135–3191

8. PERFORMING ORGANIZATION REPORT NUMBER

E–10732

9. SPONSORING/MONITORING AGENCY NAME(S) AND ADDRESS(ES)

National Aeronautics and Space Administration
Washington, DC 20546–0001
and
U.S. Army Research Laboratory
Adelphi, Maryland 20783–1145

10. SPONSORING/MONITORING AGENCY REPORT NUMBER

NASA TM–107451
ARL–TR–1370

11. SUPPLEMENTARY NOTES

F.L. Litvin and J. Lu, University of Illinois at Chicago, Chicago, Illinois 60680 (work funded under NASA Grant NAG3–1822); D.P. Townsend, NASA Lewis Research Center; and M. Hawkins, Allison Engine Company, Indianapolis, Indiana 46206. Responsible person, D.P. Townsend, organization code 5950, (216) 433–3955.

12a. DISTRIBUTION/AVAILABILITY STATEMENT

Unclassified - Unlimited
Subject Category 37

This publication is available from the NASA Center for AeroSpace Information, (301) 621–0390.

12b. DISTRIBUTION CODE

13. ABSTRACT ***(Maximum 200 words)***

An approach is proposed for computerized simulation of meshing of aligned and misaligned involute helical gears. Algorithms for TCA (Tooth Contact Analysis) computer programs were developed. Influence of misalignment on the shift of the bearing contact and transmission errors has been investigated. Numerical examples that illustrate the developed theory are provided.

14. SUBJECT TERMS

Gear; Geometry; TCA; Transmission error; Helical; Spiral bevel; Hypoid

15. NUMBER OF PAGES
22

16. PRICE CODE
A03

17. SECURITY CLASSIFICATION OF REPORT	18. SECURITY CLASSIFICATION OF THIS PAGE	19. SECURITY CLASSIFICATION OF ABSTRACT	20. LIMITATION OF ABSTRACT
Unclassified	Unclassified	Unclassified	